

Inorganic–Organic Hybrid Polymers by Polymerization of Methacrylate- or Acrylate-Substituted Oxotitanium Clusters with Methyl Methacrylate or Methacrylic Acid

Bogdan Moraru, Nicola Hüsing, Guido Kickelbick, and Ulrich Schubert*

*Institut für Materialchemie, Technische Universität Wien,
Getreidemarkt 9, A-1060 Wien, Austria*

Peter Fratzl

*Erich Schmid Institut der Österreichischen Akademie der Wissenschaften &
Montanuniversität Leoben, Jahnstrasse 12, A-8700 Leoben, Austria*

Herwig Peterlik

Institut für Materialphysik, Universität Wien, Boltzmanngasse 5, A-1090 Wien, Austria

Received January 14, 2002. Revised Manuscript Received March 18, 2002

Inorganic–organic hybrid polymers were prepared by radical polymerization of methacrylic acid or methyl methacrylate with 0.5–2 mol % of the (meth)acrylate-substituted oxotitanium clusters $Ti_6O_4(OEt)_8(OMc)_8$ (OMc = methacrylate), $Ti_6O_4(OPr)_8(OAc)_8$ (OAc = acrylate), and the new clusters $Ti_4O_2(OPr^i)_6(OOCR)_6$ ($OOCR$ = methacrylate or acrylate). A small cluster proportion is sufficient for an efficient cross-linking of the polymers. Glassy (PMMA) or powdery polymers (PMA) were obtained. With an increasing proportion of cluster, the surface area of the PMA powders increased considerably. The obtained hybrid polymers exhibit a higher thermal stability than the parent polymers because the thermal depolymerization is inhibited or at least retarded. The swelling index of cluster-cross-linked PMMA in organic solvents correlates with the cluster proportion. Small-angle scattering investigations showed that $Ti_6O_4(OPr)_8(OAc)_8$ in PMMA and PMA and $Ti_4O_2(OPr^i)_6(OMc)_6$ in PMA is more evenly distributed than $Ti_4O_2(OPr^i)_6(OMc)_6$ in PMMA. In the latter polymer, the clusters appear to aggregate and to exhibit a kind of discotic structure. Size and/or shape of the clusters and the number of polymerizable surface groups per cluster play a small but significant role in the fine-tuning of the polymer structure and the properties of the hybrid polymers.

Introduction

The basic idea behind the development of inorganic–organic hybrid materials is the combination of inorganic and organic moieties on a molecular scale to achieve a synergistic combination of the properties typical of each of the constituents. The organic and inorganic constituents may be just physically mixed, or they can be connected with each other by strong covalent or ionic bonds. Modification of the kind and proportions of the organic and inorganic constituents and their mutual arrangement allows, in principle, a deliberate tailoring of the materials properties.

One of the most versatile methods for the preparation of inorganic–organic hybrid materials of the second type is sol–gel processing, which allows the formation of the inorganic entities starting from molecular precursors. There are three approaches to prepare such hybrid materials:

1. Formation from compounds of the type $[(RO)_nM]_xY$, in which Y is an organic group or polymer chain linking two ($x = 2$) or more ($x > 2$) metal alkoxide units $[M(OR)_n]^1$. The inorganic structures are formed by sol–gel processing of the $M(OR)_n$ groups.

2. Preformation of functionalized inorganic building blocks by sol–gel processing, which are then cross-linked by polymerization of organic functions attached to the inorganic core.²

3. Formation from bifunctional molecular precursors $(RO)_nM-X-A$ bearing an inorganic $(RO)_nM$ and an organic functionality (A) capable of undergoing polymerization or cross-linking reactions.³ The hybrid polymers are formed by a combination of sol–gel processing and organic polymerization reactions.

For the development of inorganic–organic hybrid materials, the third approach is most often used. Polymers in which preformed clusters as nanosized inorganic building blocks are incorporated into organic polymers by covalent bonds (second approach) are a new

(1) Sanchez, C.; Ribot, F. *New J. Chem.* **1994**, *18*, 1007. Loy, D. A.; Shea, K. J. *Chem. Rev.* **1995**, *95*, 1431. Judeinstein, P.; Sanchez, C. *J. Mater. Chem.* **1996**, *6*, 511.

(2) Review articles: Ribot, F.; Sanchez, C. *Comments Inorg. Chem.* **1999**, *20*, 327. Kickelbick, G.; Schubert, U. *Monatsh. Chem.* **2001**, *132*, 13. Schubert, U. *Chem. Mater.* **2001**, *13*, 3487. Sanchez, C.; Soler-Illia, G. J. de A. A.; Ribot, F.; Lalot, T.; Mayer, C. R.; Cabuil, V. *Chem. Mater.* **2001**, *13*, 3061. Kickelbick, G. *Prog. Polym. Sci.*, in press.

(3) Schubert, U.; Hüsing, N.; Lorenz, A. *Chem. Mater.* **1995**, *7*, 2010.

type of inorganic–organic hybrid materials. The covalent bonding of the clusters to the organic polymer chains is achieved by using clusters substituted by polymerizable organic groups as precursors in polymerization reactions.

The only cluster type already investigated in more detail as a constituent of inorganic–organic hybrid materials are the polyhedral oligomeric silsesquioxanes (POSS), $[RSiO_{3/2}]_n$ or $R'_7RSi_8O_{12}$, and spherosilicates, $[ROSiO_{3/2}]_n$, with polymerizable groups R.⁴ Organically modified transition-metal oxide clusters (OMTOC) are the transition-metal equivalents to the POSS. In addition to the properties improvements observed for the POSS systems, the reinforcement of organic polymers by covalently bonded OMTOCs could allow interesting modifications of the optical properties of the polymers and the preparation of polymers with special magnetic or catalytic properties.

For the covalent bonding of OMTOCs to organic polymers, the organic ligands attached to the surface of the cluster core must carry a functional organic group capable of forming covalent bonds with the polymer. We have prepared a series of acrylate- or methacrylate-substituted oxotitanium and oxozirconium clusters of the general formula $M_aO_b(OH/OR)_c(OOCR)_d$ ($R'COO$ = methacrylate [OMc] or acrylate [OAc]) by reaction of $M(OR)_4$ ($M = Ti, Zr$) with (meth)acrylic acid. In these reactions, carboxylate groups first substitute one or more alkoxide ligands of $M(OR)_4$. The liberated alcohol then reacts with an excess of the acid to produce an ester and water. The water hydrolyzes the remaining alkoxide ligands and is thus the source of the oxide or hydroxide groups in the clusters. The very slow production of water allows a very controlled growth of the carboxylate-substituted oxometalate clusters. Clusters of different size and shape are obtained by controlling the alkoxide/(meth)acrylic acid ratio and the kind of OR groups in the parent alkoxide.

We have previously reported shortly on the polymerization of the clusters $Zr_6(OH)_4O_4(OMc)_{12}$ and $Zr_4O_2-(OMc)_{12}$ with methyl methacrylate as co-monomers and some of the properties of the thus-obtained cluster-cross-linked poly(methyl methacrylate) (PMMA) to demonstrate the principle.^{5,6} In the present article we describe titanium-based hybrid polymers obtained by reaction of $Ti_6O_4(OEt)_8(OMc)_8$ ⁷ and the new cluster $Ti_4O_2(OPr)_6(OMc)_6$ (and the corresponding acrylate derivatives) with methyl methacrylate and methacrylic acid. The two organic monomers were chosen to discuss some general trends; any other unsaturated organic co-monomers could be chosen as well (see ref 5e as an example).

(4) Review articles: Harrison, P. G. *J. Organomet. Chem.* **1997**, *542*, 141; Schwab, J. J.; Lichtenhan, J. D. *Appl. Organomet. Chem.* **1998**, *12*, 707.

(5) (a) Trimmel, G.; Fratzl, P.; Schubert, U. *Chem. Mater.* **2000**, *12*, 602. (b) Trimmel, G.; Gross, S.; Kickelbick, G.; Schubert, U. *Appl. Organomet. Chem.* **2001**, *15*, 401. (c) Trimmel, G.; Moraru, B.; Gross, S.; Di Noto, V.; Schubert, U. *Macromol. Symp.* **2001**, *175*, 357. (d) Gross, S.; Trimmel, G.; Schubert, U.; Di Noto, V. *Polym. Adv. Technol.* **2002**, *13*, 254. (e) Schubert, U.; Völkel, T.; Moszner, N. *Chem. Mater.* **2001**, *13*, 3811.

(6) Schubert, U.; Trimmel, G.; Moraru, B.; Tesch, W.; Fratzl, P.; Gross, S.; Kickelbick, G.; Hüsing, N. *Mater. Res. Soc. Symp. Proc.* **2001**, *628*, CC2.3.1.

(7) Schubert, U.; Arpac, E.; Glaubitt, W.; Helmerich, A.; Chau, C. *Chem. Mater.* **1992**, *4*, 291.

Experimental Section

All operations were carried out in Schlenk tubes under an argon atmosphere. The alkoxides and acids were used as-received (Aldrich). Cluster **1a** was prepared as previously reported.⁷

The specific surface areas were determined by the BET method using nitrogen adsorption at 77 K on a Micrometrics ASAP 2010. Before measurement, each sample was degassed at 50 °C under vacuum for 4 h. The specific surface areas of the samples were determined from the linear portion of the BET plots. Differential scanning calorimetry (DSC) analyses were performed on a Shimadzu TA-50 WSI thermal analyzer. The samples were heated in air with a heating rate of 5 °C/min.

Synthesis of $Ti_6O_4(OPr)_8(OAc)_8$ (1b). An amount of 2.537 g (8.9 mmol) of $Ti(OPr)_4$ was mixed with 1.433 g (19.7 mmol) of acrylic acid. The mixture was stored in a closed vessel at 4 °C. After 3 weeks, yellowish crystals of **1b** were isolated by decanting the mother liquid and drying. Yield: 1.55 g (75%). ¹H NMR ($CDCl_3$): δ 0.80–0.93 (m, 26 H, $OCH_2CH_2CH_3$), 1.55–1.63 (m, 18 H, $OCH_2CH_2CH_3$), 4.06–4.51 (m, 15 H, $OCH_2CH_2CH_3$), 5.63–5.82 (m, 8H, *cis*- $CH_2=CHCOO$), 6.04–6.19 (m, 8H, $CH_2=CHCOO$), 6.31–6.45 (m, 8H, *trans*- $CH_2=CHCOO$) ppm. ¹³C NMR ($CDCl_3$): δ 10.1 ($OCH_2CH_2CH_3$), 25.8 ($OCH_2CH_2CH_3$), 64.7 ($OCH_2CH_2CH_3$), 128.3–130.1 ($CH_2=CHCOO$), 130.5–131.8 ($CH_2=CHCOO$), 172.5–174.3 (COO) ppm. Elemental analysis found (calcd): C, 42.7 (41.4); H, 5.9 (5.8); TiO_2 , 28.4 (30.4). The methacrylate derivative $Ti_6O_4(OPr)_8(OMc)_8$ (**1c**) was prepared analogously.

Synthesis of $Ti_4O_2(OPr)_6(OMc)_6$ (2a). An amount of 3.162 g (11.1 mmol) of $Ti(OPr)_4$ was mixed with 1.894 g (26.0 mmol) of methacrylic acid. The mixture was stored in a closed vessel at 4 °C. After 3 weeks, yellowish crystals of **2a** were isolated by decanting the mother liquid and drying. Yield: 1.81 g (60%). ¹H NMR ($CDCl_3$): δ 1.17–1.25 (m, 38H, $OCH(CH_3)_2$), 1.87–1.93 (m, 25H, $CH_2=C(CH_3)COO$), 3.98–4.03 (m, 6H, $OCH(CH_3)_2$), 5.61–5.80 (m, 6H, *cis*- $CH_2=C(CH_3)COO$), 6.04–6.25 (m, 6H, *trans*- $CH_2=C(CH_3)COO$) ppm. ¹³C NMR ($CDCl_3$): δ 18.3 ($CH_2=C(CH_3)COO$), 25.3 ($OCH(CH_3)_2$), 64.4 ($OCH(CH_3)_2$), 125.8–127.9 ($CH_2=C(CH_3)COO$), 137–139.5 ($CH_2=C(CH_3)COO$), 172.8–176.8 (COO) ppm. Elemental analysis found (calcd): C, 44.2 (46.3); H, 5.9 (6.7); TiO_2 , 28.0 (29.3).

Synthesis of $Ti_4O_2(OPr)_6(OAc)_6$ (2b). An amount of 3.074 g (10.8 mmol) of $Ti(OPr)_4$ was mixed with 1.576 g (21.6 mmol) of acrylic acid. The mixture was stored in a closed vessel at 4 °C. After 3 weeks, yellowish crystals of **2b** were isolated by decanting the mother liquid and drying. Yield: 1.36 g (50%). ¹H NMR ($CDCl_3$): δ 1.16–1.25 (m, 38H, $OCH(CH_3)_2$), 3.98–4.03 (m, 6H, $OCH(CH_3)_2$), 5.79–5.83 (m, 6H, *cis*- $CH_2=CHCOO$), 6.13–6.21 (m, 6H, $CH_2=CHCOO$), 6.37–6.44 (m, 6H, *trans*- $CH_2=CHCOO$) ppm. ¹³C NMR ($CDCl_3$): δ 25.3 ($OCH(CH_3)_2$), 64.6 ($OCH(CH_3)_2$), 128.9–130.1 ($CH_2=CHCOO$), 130.7–132.9 ($CH_2=CHCOO$), 172.1–175–1 (COO) ppm. Elemental analysis found (calcd): C, 42.3 (44.7); H, 6.8 (6.4); TiO_2 , 29.5 (31.8).

X-ray Structure Analyses of **1b, **1c**, **2a**, and **2b**.** Selected crystals were mounted on a Siemens SMART diffractometer with a CCD area detector. Graphite-monochromated Mo K α radiation (71.073 pm) was used for all measurements. The crystal-to-detector distance was 4.40 cm. A hemisphere of data was collected by a combination of three sets of exposures at 213 (**1c**) or 223 K (**2**). Each set had a different ϕ angle for the crystal, and each exposure took 20 s and covered 0.3° in ω . The data were corrected for polarization and Lorentz effects, and an empirical absorption correction (SADABS) was applied. The cell dimensions were refined with all unique reflections. The structure was solved by direct methods (SHELXS86). Refinement was carried out with the full-matrix least-squares method based on F^2 (SHELXL93) with anisotropic thermal parameters for all non-hydrogen atoms. Hydrogen atoms were inserted in calculated positions and refined riding with the corresponding atom. A summary of the crystallographic data for the structures of **1b**, **1c**, **2a**, and **2b** is given in Table 1. The full data have been deposited at the Cambridge Crystal-

Table 1. Crystallographic and Structural Parameters of **1b, **1c**, **2a**, and **2b****

	1b	1c	2a	2b
empirical formula	$C_{48}H_{84}O_{28}Ti_6$	$C_{56}H_{42}O_{28}Ti_6$	$C_{42}H_{72}O_{20}Ti_4$	$C_{36}H_{60}O_{20}Ti_4$
formula weight	1396.5	1490.6	1088.6	1004.4
crystal system, space group	monoclinic, $P2_1/c$	monoclinic, $P2_1/c$	triclinic, $P\bar{1}$	monoclinic, $P2_1/c$
<i>a</i> (pm)	12,233(1)	15,919(1)	1321,91(9)	1786,1(4)
<i>b</i> (pm)	13,871(2)	13,1020(9)	20,423(1)	1022,3(3)
<i>c</i> (pm)	20,705(2)	18,4872(12)	20,751(2)	2756,6(8)
α (deg)			81,625(2)	
β (deg)	107,182(2)	105,601(1)	82,860(2)	97,44(2)
γ (deg)			85,951(2)	
volume (pm ³)	$3356.4(6) \times 10^6$	$3713.9(4) \times 10^6$	$5491.7(7) \times 10^6$	$4991(2) \times 10^6$
Z (calcd density (g·cm ⁻³)	2/1.382	2/1.333	4/1.317	4/1.337
μ (mm ⁻¹)	0.755	0.687	0.628	0.685
crystal size (mm)	0.80 \times 0.26 \times 0.16	0.6 \times 0.5 \times 0.1	0.36 \times 0.12 \times 0.07	0.4 \times 0.2 \times 0.2
2 θ range (deg)	1.74–28.54	1.93–24.71	1.90–20.81	1.76–24.74
reflections coll./unique	8458/8458	9093/6110	16742/11357	8521/8521
data/parameters	8458/371	6110/416	11357/1189	8521/542
GOF	1.057	1.030	0.941	1.037
R1 [<i>I</i> > 2 σ (<i>I</i>)]	0.0492	0.0466	0.0544	0.0368
wR2	0.1294	0.1293	0.1330	0.0946
largest diff. peak and hole (e·Å ⁻³)	0.918/–0.669	0.781/–0.517	0.592/–0.390	0.845/–0.530

Table 2. Preparation of the Hybrid Polymers and Elemental Analysis Data

cluster type (organic monomer ^a)	cluster g (mmol)	organic monomer g (mmol)	initiator g (mmol)	toluene (mL)	elemental analysis found (calcd.)		
					C	H	TiO ₂
2a (MA)	0.070 (0.06)	1.665 (19.3)	0.012 (0.05)	2	55.7 (55.4)	7.3 (9.2)	0.9 (1.2)
	0.105 (0.09)	1.678 (19.5)	0.013 (0.05)	4	54.7 (55.2)	7.2 (9.2)	1.4 (1.7)
	0.083 (0.07)	0.711 (8.3)	0.007 (0.03)	2.5	52.4 (54.7)	7.1 (6.9)	3.9 (3.3)
	0.115 (0.11)	0.541 (6.3)	0.007 (0.03)	2.5	54.1 (53.9)	7.1 (6.9)	3.9 (5.9)
2b (MA)	0.140 (0.14)	3.730 (43.3)	0.025 (0.11)	5			
	0.468 (0.46)	7.832 (90.9)	0.052 (0.21)	9			
	0.413 (0.41)	3.750 (43.5)	0.025 (0.11)	5			
	0.189 (0.19)	1.240 (14.4)	0.011 (0.05)	2			
	0.207 (0.21)	0.854 (9.91)	0.008 (0.03)	2			
1a (MA)	0.346 (0.25)	5.828 (67.0)	0.031 (0.13)	5	55.1 (54.9)	7.1 (6.9)	2.2 (1.9)
	0.387 (0.28)	4.935 (57.3)	0.031 (0.13)	5	53.3 (54.8)	7.1 (6.9)	2.8 (2.5)
	0.444 (0.32)	4.315 (50.1)	0.024 (0.10)	5	52.1 (53.8)	6.9 (6.9)	3.9 (4.6)
	0.779 (0.56)	2.497 (29.0)	0.026 (0.11)	5	51.7 (52.1)	6.4 (6.7)	8.7 (8.1)
1b (MA)	0.145 (0.10)	2.520 (29.3)	0.026 (0.11)	4	55.1 (54.9)	7.1 (6.9)	2.2 (1.9)
	0.149 (0.11)	1.881 (21.8)	0.020 (0.08)	4	53.3 (54.8)	7.1 (6.9)	2.8 (2.5)
	0.164 (0.12)	1.182 (13.7)	0.016 (0.07)	4	52.1 (53.8)	6.9 (6.9)	3.9 (4.6)
	0.276 (0.20)	0.920 (10.7)	0.016 (0.07)	4	51.7 (52.1)	6.4 (6.7)	8.7 (8.1)
2a (MMA)	0.057 (0.05)	1.091 (10.9)	0.012 (0.05)	4	60.6 (59.3)	8.2 (9.9)	1.4 (1.5)
	0.106 (0.10)	1.020 (10.2)	0.014 (0.06)	2.5	59.5 (58.7)	8.1 (9.7)	2.1 (2.8)
	0.119 (0.11)	0.650 (6.5)	0.014 (0.06)	2.5	57.3 (57.8)	7.7 (9.5)	4.7 (4.6)
2b (MMA)	0.088 (0.09)	2.779 (27.7)	0.027 (0.11)	5			
	0.131 (0.13)	2.852 (28.5)	0.027 (0.11)	5			
	0.198 (0.19)	3.259 (32.6)	0.031 (0.13)	5			
	0.309 (0.31)	3.134 (31.3)	0.011 (0.05)	5			
1a (MMA)	0.088 (0.06)	6.455 (62.3)	0.048 (0.20)	7			
	0.189 (0.14)	4.122 (40.3)	0.030 (0.12)	5	61.1 (59.2)	8.1 (8.0)	1.3 (1.5)
	0.190 (0.14)	2.941 (28.8)	0.021 (0.09)	5			
	0.356 (0.26)	4.025 (39.4)	0.029 (0.12)	5			
	0.395 (0.28)	2.958 (29.5)	0.021 (0.09)	5	57.5 (57.4)	7.7 (7.7)	3.5 (4.1)
	0.409 (0.29)	1.507 (14.7)	0.029 (0.12)	5	59.7 (55.8)	7.5 (7.5)	6.2 (7.5)
1b (MMA)	0.102 (0.07)	1.491 (14.9)	0.021 (0.08)	3			
	0.194 (0.14)	1.390 (13.9)	0.035 (0.14)	3			
	0.230 (0.16)	0.820 (8.2)	0.025 (0.10)	3			

^a MA = methacrylic acid; MMA = methyl methacrylate.

lographic Data Centre as supplementary publication no. CCDC 167592 (**1b**), CCDC 167595 (**1c**), CCDC 167594 (**2a**), and CCDC 167593 (**2b**). Copies of the data can be obtained free of charge on application to CCDC, 12 Union Road, Cambridge CB2 1EZ, U.K. (Fax +44-1223/336-033; e-mail deposit@ccdc.cam.ac.uk).

Preparation of the Hybrid Polymers. Radical-initiated polymerization of the clusters **1** and **2** with a 50- to 300-fold molar excess of methyl methacrylate as co-monomer in toluene at 65 °C for 12 h, with dibenzoylperoxide as initiator (Table 2), gave glassy polymers with methyl methacrylate, which still

contained some solvent after drying at reduced pressure for 8 h, while polymerization with methacrylic acid under the same conditions leads to white to yellowish powders. The residual solvent in the glassy PMMA polymers was removed by extraction with ethyl acetate. Elemental analyses (Table 2) showed that the polymers were essentially solvent-free after this treatment.

Small-Angle Scattering (SAXS). The measurements were performed using a pinhole camera with a rotating anode generator (Ni-monochromated Cu K α radiation) and an area detector (Bruker AXS, Karlsruhe). All SAXS patterns were

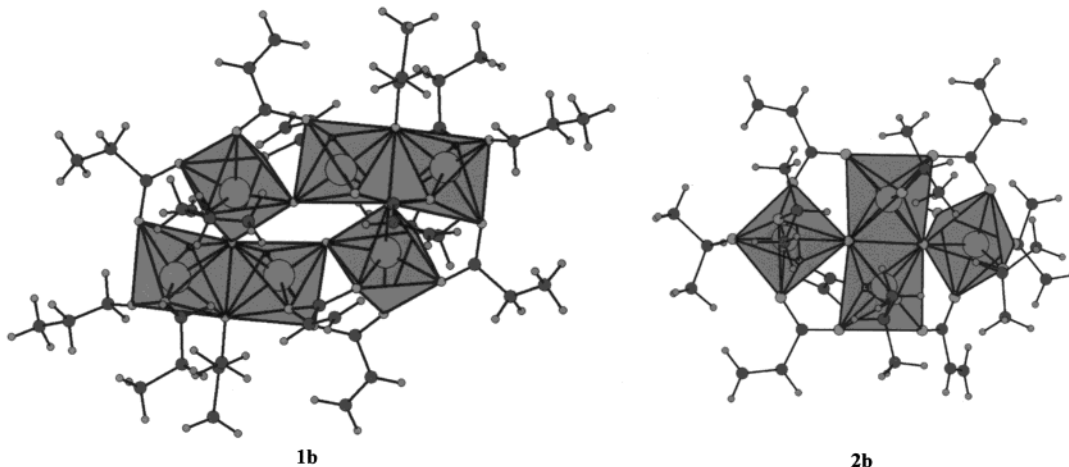


Figure 1. Molecular structures of $\text{Ti}_6\text{O}_4(\text{OPr})_8(\text{OAc})_8$ (**1b**) and $\text{Ti}_4\text{O}_2(\text{OPr})_6(\text{OAc})_6$ (**2b**).

first corrected for background scattering from the experimental setup and then radially averaged to obtain the function $I(q)$, where $q = (4\pi/\lambda) \sin \theta$ is the scattering vector, 2θ being the angle between the incident and the diffracted beam, and $\lambda = 0.154$ nm the X-ray wavelength. Scattering curves were obtained in the q range $0.15\text{--}9$ nm $^{-1}$ by combining data measured for two different sample-detector distances.

Results and Discussion

Preparation and Characterization of the (Meth)acrylate-Substituted Clusters. When transition-metal alkoxides are reacted with a particular carboxylic acid, three parameters influence the type of the formed cluster: (i) the kind of carboxylic acid, (ii) the kind of alkoxide groups, and (iii) the employed metal/carboxylic acid molar ratio.

- Two methacrylate-substituted titanium polyoxoalkoxides were previously prepared by reaction of titanium *n*-alkoxides with methacrylic acid, that is, $\text{Ti}_6\text{O}_4(\text{OEt})_8(\text{OMc})_8$ (**1a**)⁷ and $\text{Ti}_9\text{O}_8(\text{OPr})_4(\text{OMc})_{16}$.⁸ Cluster **1a** was obtained when 2 molar equiv of methacrylic acid were reacted with $\text{Ti}(\text{OEt})_4$ and the Ti_9 cluster from 4 equiv of methacrylic acid and $\text{Ti}(\text{OPr})_4$.

- The same cluster type as **1a**, $\text{Ti}_6\text{O}_4(\text{OPr})_8(\text{OOCR})_8$, was formed when $\text{Ti}(\text{OPr})_4$ was reacted with 2.2–2.3 molar equiv of acrylic or methacrylic acid (**1b**, $\text{Ti}_6\text{O}_4(\text{OPr})_8(\text{OAc})_8$; **1c**, $\text{Ti}_6\text{O}_4(\text{OPr})_8(\text{OMc})_8$); that is, the (small) difference between acrylic and methacrylic acid and between OEt and O^nPr does not influence the type of formed cluster.

- A new cluster type, $\text{Ti}_4\text{O}_2(\text{O}^i\text{Pr})_6(\text{OOCR})_6$ (**2a**, RCOO = methacrylate; **2b**, RCOO = acrylate), was obtained when $\text{Ti}(\text{O}^i\text{Pr})_4$ was reacted with 2 equiv of either acrylic or methacrylic acid. This shows that the steric bulk of the alkoxide group in the parent metal alkoxide influences the type of obtained cluster (for another example see ref 9). This can be due to the bulkiness of the alkoxide ligands or to the degree of association of the parent alkoxide. Note that $\text{Ti}(\text{OEt})_4$ and $\text{Ti}(\text{OPr})_4$ are trimeric in solution, while $\text{Ti}(\text{O}^i\text{Pr})_4$ is monomeric because of its larger alkoxide groups.

The Ti_4 clusters **2a,b** are distinctly less soluble in toluene (which was used for the polymerization reac-

tions described below) than **1a,b**. The solubility also depends on the alkoxide ligands since **1b** (OPr ligands) has a higher solubility than **1a** (OEt ligands). The solubility of the used clusters in toluene thus decreases in the order **1b** > **1a** >> **2a,b**.

The molecular structure of **1a** was previously published,⁷ and the molecular structures of $\text{Ti}_6\text{O}_4(\text{OPr})_8(\text{OAc})_8$ (**1b**) and $\text{Ti}_4\text{O}_2(\text{OPr})_6(\text{OAc})_6$ (**2b**) are shown in Figure 1. The methacrylate clusters **1a**, **1c**, and **2a** (not shown) are isostructural with the corresponding acrylate derivatives. The particular representation of the structures in Figure 1 was chosen to show the linkage of the $[\text{TiO}_6]$ octahedra as well as the coverage of the cluster cores with the polymerizable ligands. The common structural motif of both structures is the same as the basic structural unit of rutile, for example, a group of three octahedra, two of them sharing an edge, with one corner of the third octahedron is connected to this edge via a μ_3 -oxygen. In **1**, two of these groups make up the Ti_6 unit, while in **2** a single octahedron is condensed to the Ti_3 unit via a second μ_3 -oxygen. The (meth)acrylate ligands are exclusively bridging in each case, as has been found for other carboxylate-substituted oxotitanium clusters.

The structure of **2** is very similar to that of $\text{Zr}_4\text{O}_2(\text{OMc})_{12}$,^{5b,10} with the difference being that the inner zirconium atoms are seven-coordinate and the outer zirconium atoms are eight-coordinate. Because a smaller number of coordination sites are available in the titanium clusters **2**, the degree of substitution of the (monodentate) alkoxide groups by (bidentate) carboxylate groups is lower.

The main reason for investigating both the acrylate and the methacrylate derivative of **1** and **2** as building blocks for inorganic–organic hybrid materials was to check the influence of substituent effects (OMc vs OAc; ^iPrO vs ^nPrO and EtO) on the materials properties.

Polymerization with Methacrylic Acid as Comonomer. Radical-initiated polymerization of 0.3–2.0 mol % of the clusters **1a,b** and **2a,b** with methacrylic acid in toluene at 65 °C, with dibenzoylperoxide as the initiator, resulted in white to yellowish powders. The ^{13}C CP-MAS NMR spectra of the resulting polymers showed intense peaks for the polymerized methacrylic

(8) Kickelbick, G.; Schubert, U. *Eur. J. Inorg. Chem.* **1998**, 159, 9.
(9) Moraru, B.; Kickelbick, G.; Schubert, U. *Eur. J. Inorg. Chem.* **2001**, 1295.

(10) Kickelbick, G.; Schubert, U. *Chem. Ber.* **1997**, 130, 473.

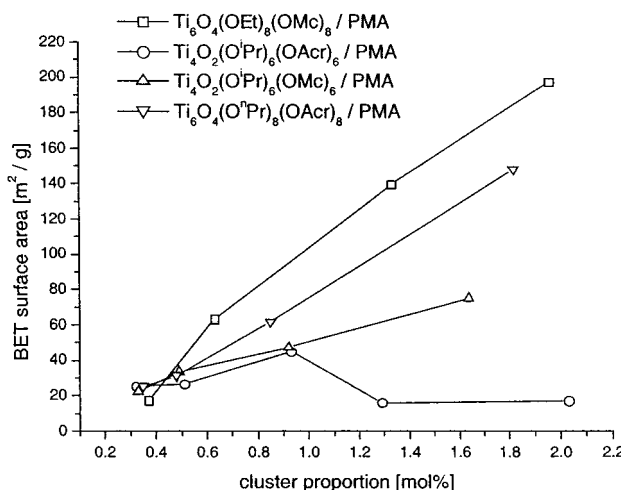


Figure 2. BET surface areas vs molar monomer/cluster ratio (r_d) for methacrylic acid copolymerized with the titanate clusters **1a,b** and **2a,b**.

acid (at 17.6 [CH_3], 45.3 [CMe], 54.9 [CH_2], and 184.9 ppm [COO]) and additional two low-intensity signals at 129 and 136 ppm. The latter are ascribed to unreacted vinylic CH_2 groups. However, because the CH_2 signals of methacrylic acid and the clusters **1** and **2** have very similar chemical shifts, the residual peaks in the MAS NMR spectra cannot be assigned to either of these groups.

With a low cluster proportion, the BET surface area of the hybrid polymers was about that of undoped poly(methacrylic acid) (PMA) ($12 \text{ m}^2/\text{g}$) prepared under the same conditions. With an increasing proportion of cluster, the surface area increased considerably (Figure 2), and surface areas up to $200 \text{ m}^2/\text{g}$ were obtained with as little as 2 mol % of cluster. The isotherms were of type II (according to IUPAC¹¹), which is characteristic of nonporous or macroporous materials. Because the pore volumes calculated by the BET method and the BJH method (Barrett–Joyner–Halenda) were nearly the same, the materials contain no micropores. With the exception of PMA doped by the cluster **2b**, there was an approximately linear dependence between the BET surface area and the cluster proportion in the investigated range. There are two significant trends: (i) the BET surface areas of PMA cross-linked by the methacrylate derivatives **1a** and **2a** are higher than those of the corresponding acrylate clusters **1b** and **2b** and (ii) the BET surface areas of PMA cross-linked by the Ti_6 clusters **1a** and **1b** are higher than those of the corresponding Ti_4 clusters **2a** and **2b**. A possible interpretation of these findings could be that the larger size of the Ti_6 clusters and the size of the methyl group in the methacrylate derivatives result in more open polymer network structures. In the PMMA polymers cross-linked by >1 mol % of **2b**, we observed X-ray reflections above in the wide-angle region. Although we have currently no explanation for this crystallization phenomenon, it may be the reason for the low surface area of these polymers (Figure 2).

While undoped PMA dissolves in water, the cluster-cross-linked polymers were insoluble. In a water-

saturated atmosphere they slowly took up water (about 0.15–0.3 g of water/g of polymer within several days). However, contrary to the solvent uptake of cluster-cross-linked PMMA (see below), there was no clear dependence on the cluster proportion.

DSC of undoped PMA shows an endothermic event at about 230°C (Figures 3 and 4). This could be due to depolymerization reactions and/or melting transitions. A concomitant weight loss of about 15% at the same temperature in TGA (not shown) shows that depolymerization plays at least some role. The depolymerization or melting transition at 230°C is suppressed or eliminated when the polymer is cross-linked by the clusters. In general, the intensity of the DSC signal at 230°C decreased as the cluster proportion was increased. When PMA was cross-linked by the clusters **1a** or **1b** (Figure 3), this thermal event was completely suppressed with a cluster proportion of about 2 mol %, while with 2 mol % of the clusters **2a** or **2b** (Figure 4) it was just reduced. This result shows that the cross-linking efficiency of **2** is smaller than that of **1**. At higher temperatures, the polymers were oxidatively degraded (the experiments were performed in air). The mass of the solid residues in the TGA experiments upon heating the polymers to 800°C corresponds very well to the TiO_2 content.

Polymerization with Methyl Methacrylate as Co-monomer. Radical-initiated polymerization of 0.1–2.0 mol % of **1a,b** and **2a,b** with methyl methacrylate in toluene under the same conditions gave yellowish glasses without measurable surface areas. The glasses still contained some solvent after drying at reduced pressure, which was removed by extraction with ethyl acetate. As in the case of cluster-doped PMA, weak signals of unreacted double bonds were observed in the ^{13}C CP-MAS NMR spectra.

While undoped PMMA dissolves in various organic solvents, the cluster-cross-linked polymers only swelled. The solvent uptake per gram of the polymer after storage in ethyl acetate for 3 days is shown in Figure 5. The swelling behavior of the cluster-reinforced PMMA in ethyl acetate depended clearly on the cluster proportion. This relationship clearly shows that the cross-linking density increases with an increasing proportion of the cluster. A similar behavior was already observed for PMMA cross-linked by oxozirconium clusters.⁵ Interestingly, the swelling of the polymers depended on the type of incorporated cluster. The clusters **2a,b** had a distinctly lower cross-linking efficiency than **1a,b**. One of the reasons for this behavior could be the smaller number of (meth)acrylate ligands per cluster. However, even if the swelling is scaled to the number of cluster-bonded (meth)acrylate ligands, the cross-linking efficiency of **2** is still smaller than that of **1**, as already noted above for the thermal stability studies. Another reason could be the different spatial distribution of the (meth)acrylate ligands due to the different geometry of the cluster cores. There is no significant difference between the acrylate and methacrylate derivatives.

The clusters **1** and **2** are moisture-sensitive. Nevertheless, the cluster-cross-linked polymers were stable at ambient atmosphere even for prolonged periods, and their properties did not change. Particularly, the glassy, transparent PMMA polymers did not get turbid. This

(11) Sing, K. S.; Everett, D. H.; Aul, R. A. W.; Moscou, L.; Pierotti, R. A.; Rouquerol, J.; Siemieniewska, T. *Pure Appl. Chem.* **1985**, *57*, 603.

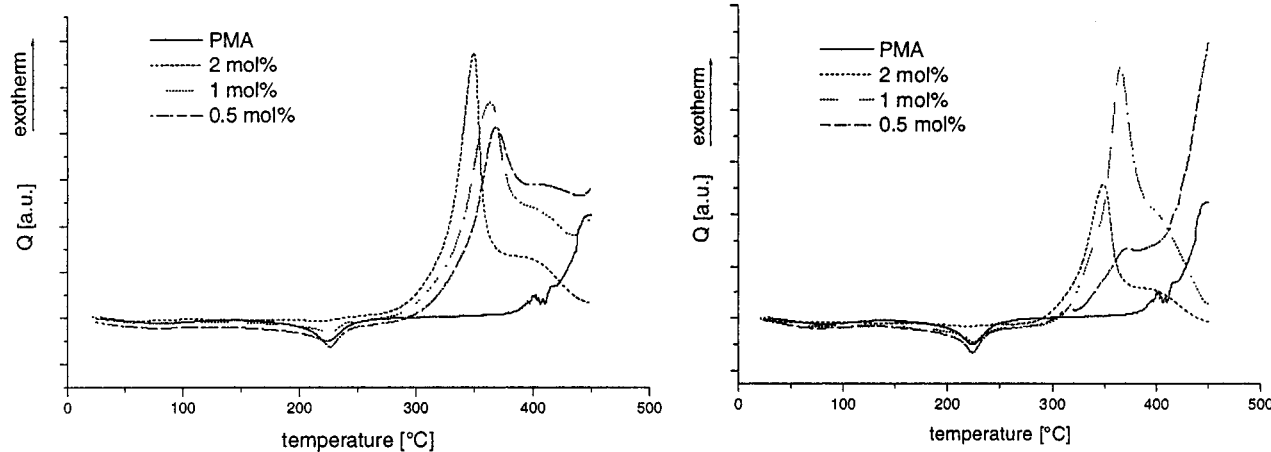


Figure 3. DSC (in air) of undoped PMA and PMA cross-linked by cluster **1a** (left) and **1b** (right).

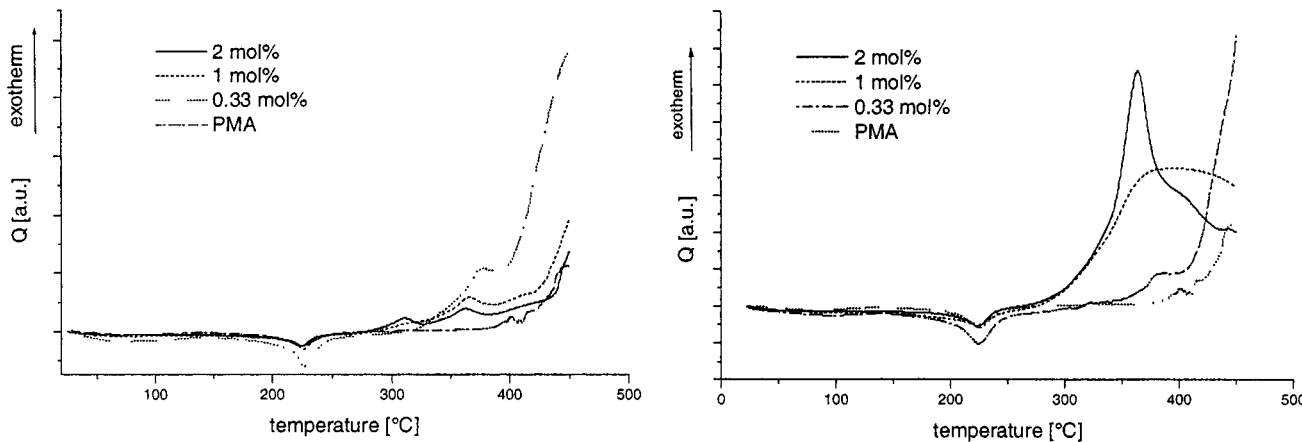


Figure 4. DSC (in air) of undoped PMA and PMA cross-linked by cluster **2a** (left) and **2b** (right).

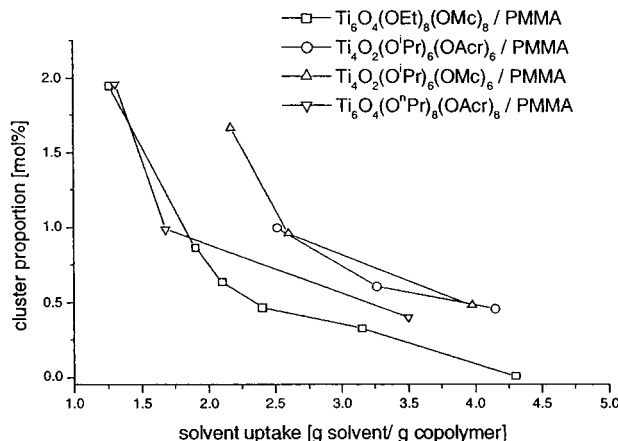


Figure 5. Swelling of the cluster-cross-linked PMMA after storage in ethyl acetate for 3 days.

indicates that the clusters are either protected against hydrolysis once incorporated into the polymer or do not form larger titania particles after hydrolysis.

The thermal behavior of cluster-cross-linked PMMA is very similar to that of cluster-cross-linked PMA, except for the fact that a smaller proportion of the cluster is sufficient to suppress the depolymerization reaction. Undoped PMMA decomposes above 330 °C. The thermal behavior of PMMA cross-linked by 0.3 mol % of **1a** was investigated in more detail and is reported in a follow-up paper.¹² The mass of the solid residues in the TGA experiments upon heating the polymers to

800 °C again corresponded very well to the TiO₂ content. (PMMA doped by 1 mol % of the clusters contains 4.2 wt % of TiO₂ when cross-linked by **1a** and 2.9 wt % of TiO₂ when cross-linked by **2a**.)

Small-Angle Scattering (SAXS). The SAXS data for PMMA cross-linked by 0.5, 1, and 2 mol % of **2a** are shown in Figure 6. SAXS data were obtained for three different mole fractions of clusters (triangles, circles, and squares in Figure 6) and, in addition, measurements were carried out at three different positions within each specimen. The data were first normalized by multiplication with a factor to the same value at $q = 9 \text{ nm}^{-1}$ to obtain coincidence with the data of undoped PMMA prepared under the same conditions (Figure 6a). The underlying assumption is that, at higher q , the signal is dominated by the scattering from the PMMA matrix in each sample. Then, the scattering curve from undoped PMMA was subtracted from each of the data sets to yield the scattering from the clusters alone (Figure 6b). Because of this subtraction procedure, the data for $q > 6 \text{ nm}^{-1}$ in Figure 6b are uncertain and should be disregarded.

The scattering intensity clearly depended on the cluster proportion: as expected, the polymer with the smallest proportion of the cluster (0.5 mol %) gave the weakest signals. Moreover, there was a considerable variation in the data from each of the specimens. While

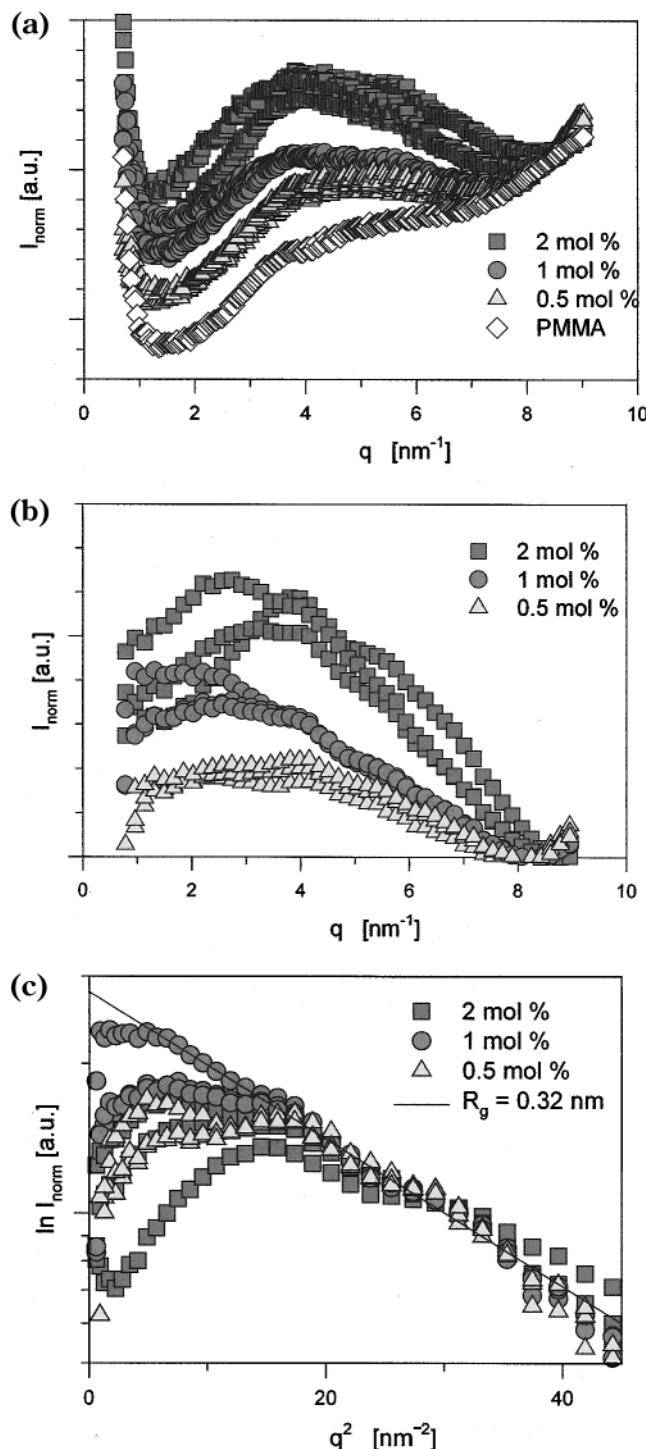


Figure 6. SAXS data of PMMA cross-linked with **2a**. (a) Original data after background correction. (b) After subtraction of PMMA. (c) Guinier plot.

our previous studies on PMMA cross-linked by oxozirconium clusters^{5,6} had revealed only one maximum of the scattering curve, the PMMA polymer cross-linked by **2a** surprisingly showed two maxima or shoulders at about $q = 4$ and 2.5 nm⁻¹ (Figure 6b). In some of the data sets, both maxima appeared very clearly and in others only one of the maxima was visible, but there was no significant shift when the cluster proportion was changed. This indicates that the clusters aggregate to some extent (clusters of clusters). When a higher proportion of methyl methacrylate co-monomer was

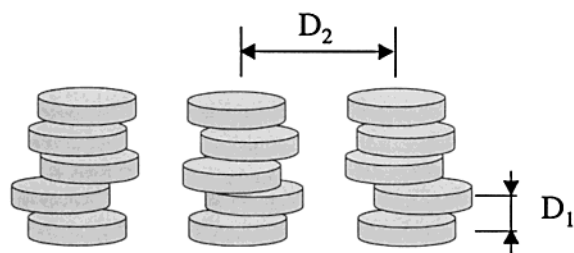


Figure 7. Sketch of a possible discotic arrangement of flat clusters in PMMA. For the cluster **2a** (Figure 6) $D_1 \approx 1.6$ nm and $D_2 \approx 2.5$ nm independently of the cluster concentration. For the cluster **1b**, $D_1 \approx 1.7$ nm independently of the cluster concentration, while D_2 increased with dilution ($D_2 \approx 2.5$ nm for 2 mol %, $D_2 \approx 3$ nm for 1 mol % of cluster).

employed in the polymerization reaction, the intercluster distance was not increased, but instead additional organic monomer was apparently incorporated between the cluster aggregates.

We can only hypothesize about the origin of the double maximum, which corresponds to different intercluster distances (about 1.6 and 2.5 nm). The first possibility is that there are two types of aggregates with different intercluster distances. A second, more likely possibility is that the anisotropic shape (elongated disks) of the clusters (see Figure 1) results in a kind of discotic arrangement of the clusters within the aggregates. The shorter distance would then correspond to the intercluster distances within a pile of disks and the longer distance to the distance between clusters of neighboring piles (see Figure 7).

Figure 6c is the Guinier plot of the data from Figure 6b. At high q^2 , the data of the different samples coincided. This shows that the cluster size is the same in all samples, as expected. From the slope of this region, the radius of gyration (R_g) was calculated as 0.32 nm. This corresponds to a disk with a diameter of about 0.9 nm, which is in good agreement with the structure of **2a**. (This diameter is the effective diameter of the clusters, where all elements have to be weighted with their respective number of electrons.)

The SAXS data of PMMA cross-linked by **1b** were treated in the same way as described above and are shown in Figure 8. The scattering data taken at three different regions of the sample were again somewhat different, indicating an inhomogeneous composition of the samples. The radius of gyration was slightly larger (0.33 nm). Again, two maxima (or shoulders) are visible in each data set. Contrary to PMMA cross-linked by **2a**, the position of the left maximum shifted to higher q with an increasing proportion of the cluster. This indicates that the clusters **1b** are more evenly distributed (less aggregated) in the polymer than the clusters **2a** because the intercluster distance increases with the methyl methacrylate proportion. Interestingly, the second maximum (well visible in the sample with 1 mol % of the cluster and as a shoulder in the samples with 0.5 and 2 mol %) did not shift with composition. The intercluster distance calculated from the maximum at large q is about 1.3 nm. The peak at small q corresponds to 2.5 and 3 nm for 2 and 1 mol % of cluster, respectively. This could again indicate some discotic structure, which, however, is less pronounced than that for **2a** in PMMA (see Figure 7). The general shape of the SAXS curves

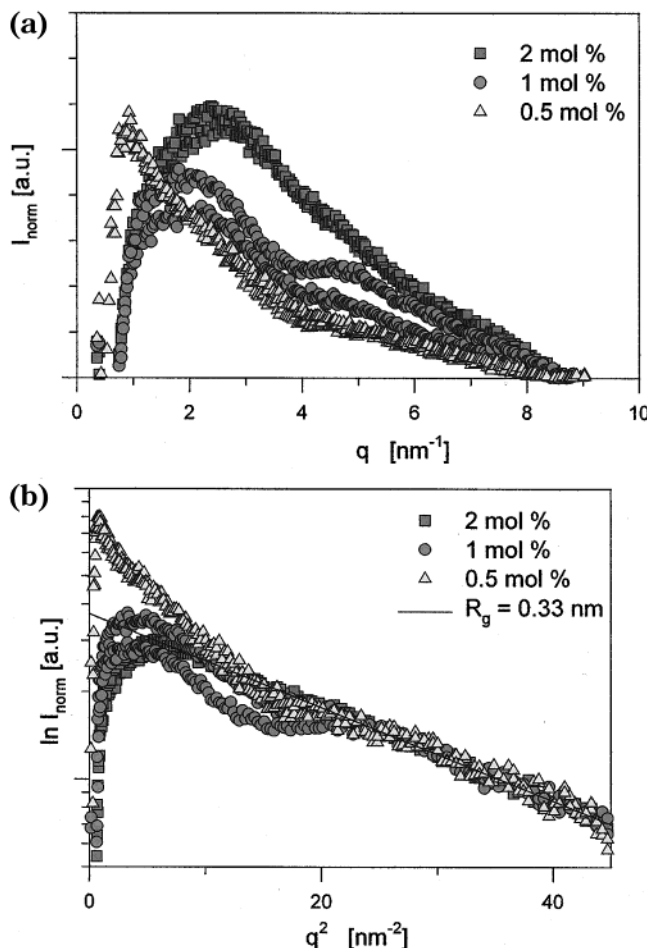


Figure 8. SAXS data of PMMA cross-linked with **1b**. (a) Data after background correction and subtraction of PMMA. (b) Guinier plot.

is similar to those already reported for PMMA cross-linked by **1a**,⁶ that is, the different carboxylate and alkoxide groups have little influence on the structure of the polymer.

The SAXS data of the PMA-based polymers cross-linked by **1b** or **2a** (Figures 9 and 10) are more difficult to interpret because the high inner and outer surface area of the powders gives rise to a much higher small-angle scattering of the undoped polymer. The surface scattering was corrected by fitting the curves in the very small q region with $I_{\text{SAXS}}(q) = Aq^{-4}$, where A is the Porod constant. Because of the subtraction of surface scattering, the data are less accurate than those for the PMMA, particularly in the small- q region.

The scattering data of PMA cross-linked by **2a**, taken at three different regions of the sample, did not differ significantly and were therefore averaged. Contrary to **2a** in PMMA, there was only one maximum in the scattering curve (Figure 9). It did not shift significantly when the cluster proportion was changed. (The small shift of the sample with the lowest cluster proportion may be due to the lower accuracy of the data in the small- q region.)

The scattering data of PMA cross-linked by **1b**, taken at three different regions of the sample, were only different for the sample containing 2 mol % of the cluster, while the samples with 1 and 0.5 mol % cluster were homogeneous. The three sets of SAXS data of the

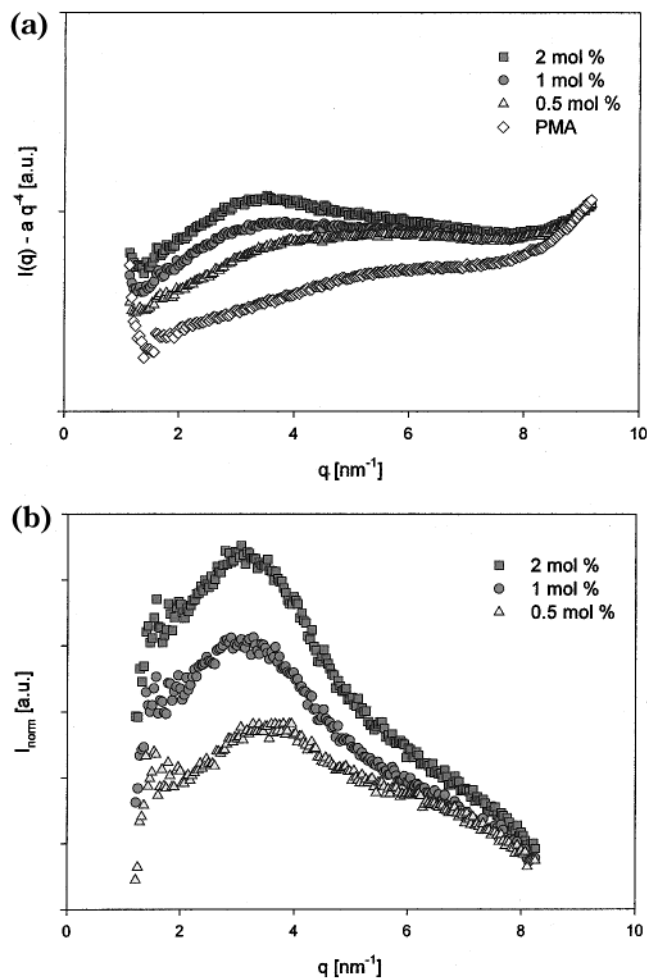


Figure 9. SAXS data of PMA cross-linked with **2a**. Data before (a) and after (b) subtraction of PMA.

latter two samples were therefore averaged. The resulting SAXS curves are shown in Figure 10. Despite the lower accuracy of the data, a shift of the scattering maximum to smaller q was clearly observed when the cluster proportion in the polymer was decreased. This behavior is expected when the clusters are homogeneously distributed in the polymer.

Conclusions

The preparation of the new inorganic–organic polymers described in this article is basically a two-step process. In the first step, the oxotitanium clusters **1** and **2** are prepared by carefully controlled hydrolysis of (meth)acrylate-substituted $\text{Ti}(\text{OR})_4$. The type of formed cluster depends on the steric bulk of the alkoxide ligand (OR) of the employed $\text{Ti}(\text{OR})_4$ for a given $\text{Ti}(\text{OR})_4$ /carboxylic acid ratio, while the acid (acrylic or methacrylic acid) has no influence. The isolated clusters are then polymerized with methacrylic acid or methyl methacrylate as co-monomers, and glassy (PMMA) or powdery polymers (PMA) are obtained. The clusters can be considered structurally well-defined (i.e., monodispersed) metal oxide nanoparticles, which are incorporated in the polymer network via surface-bonded organic groups. Owing to the large number of (meth)acrylate ligands, the clusters cross-link the polymer chains very efficiently, even if only a small proportion of the clusters is employed.

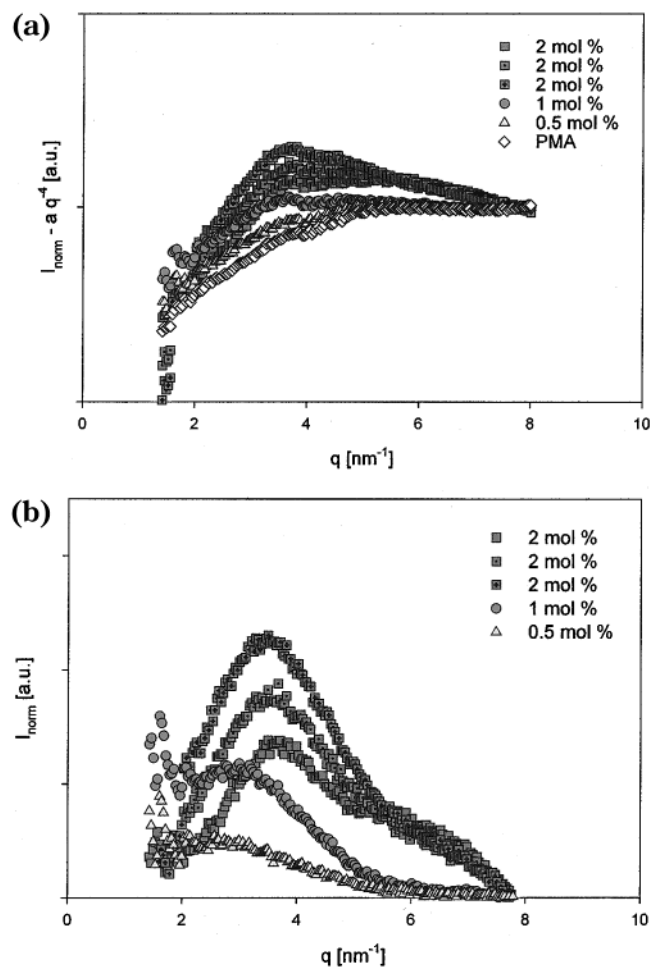


Figure 10. SAXS data of PMA cross-linked with **1b**. Data before (a) and after (b) subtraction of PMA.

The surface area of the cluster-cross-linked PMA powders is increased when the cluster proportion in the polymer is increased. With only 2 mol % of the cluster, high surface areas—up to $200 \text{ m}^2/\text{g}$ —are obtained. The crystallization phenomenon observed for PMA doped with $>1 \text{ mol } \%$ of **2b** can currently not be explained.

A number of polymer properties are changed by the cluster cross-linking. The thermal properties are improved because the thermal depolymerization of PMMA or PMA is prevented or at least inhibited. Cluster-cross-linked PMMA swells in contact with organic solvents; the solvent uptake correlates with the cluster proportion, that is, the degree of cross-linking. The mechanical properties of PMMA cross-linked by 0.3 mol % of **1a** are greatly improved, as will be reported in a follow-up paper.¹¹

The SAXS data show that cluster **1b** is homogeneously dispersed both in PMMA and PMA; the mean cluster–cluster distance increases as the proportion of the cluster in the polymer is decreased. This model can no longer be applied for PMMA cross-linked with cluster **2a**. The SAXS curves have two maxima, which can be explained by the assumption of a kind of discotic arrangement of the clusters with shorter intercluster distances within a pile of disks and longer distances between clusters of neighboring piles. PMA cross-linked with cluster **2a** did not show this phenomenon. However, the intercluster distance did not significantly depend on the cluster proportion in the polymer, indicating some clustering of the clusters. The reason for the different arrangement of the clusters in the polymer could be a more anisotropic shape of **2a** (a flatter oblate spheroid) compared to that of **1b**.

The results presented in this paper show that some modulation of the properties is achieved by the kind of employed clusters. Size and/or shape of the clusters and the number of polymerizable surface groups per cluster obviously play a small but significant role in the fine-tuning of the polymer structure and the properties of the hybrid polymers.

Acknowledgment. This work was supported by the Fonds zur Förderung der wissenschaftlichen Forschung (FWF) and the Jubiläumsfonds der Stadt Wien.

CM021113F